Thin Solid Films 518 (2010) 2365–2369

Contents lists available at ScienceDirect

Thin Solid Films

journal homepage: www.elsevier.com/locate/tsf

Evolution of SiO_2/Ge/HfO_2(Ge) multilayer structure during high temperature annealing

D. Sahin [a,*], I. Yildiz [a,b], A.I. Gencer [a], G. Aygun [c], A. Slaoui [d], R. Turan [a]

[a] Department of Physics, Middle East Technical University, TR-06531 Ankara, Turkey
[b] Central Laboratory, Middle East Technical University, TR-06531 Ankara, Turkey
[c] Department of Physics, Izmir Institute of Technology, Urla, TR-35430 Izmir, Turkey
[d] InESS-CNRS-ULP, 23 rue du Loess, F-67037 Strasbourg, France

ARTICLE INFO

Available online 13 October 2009

Keywords:
Ge
Segregation
HfO_2
XPS
Depth profiling
Raman spectroscopy

ABSTRACT

Use of germanium as a storage medium combined with a high-k dielectric tunneling oxide is of interest for non-volatile memory applications. The device structure consists of a thin HfO_2 tunneling oxide with a Ge layer either in the form of continuous layer or discrete nanocrystals and relatively thicker SiO_2 layer functioning as a control oxide. In this work, we studied interface properties and formation kinetics in SiO_2/Ge/HfO_2(Ge) multilayer structure during deposition and annealing. This material structure was fabricated by magnetron sputtering and studied by depth profiling with XPS and by Raman spectroscopy. It was observed that Ge atoms penetrate into HfO_2 layer during the deposition and segregate out with annealing. This is related to the low solubility of Ge in HfO_2 which is observed in other oxides as well. Therefore, Ge out diffusion might be an advantage in forming well controlled floating gate on top of HfO_2. In addition we observed the Ge oxidation at the interfaces, where $HfSiO_x$ formation is also detected.

1. Introduction

Integrated circuit technology is looking for potential materials to replace SiO_2 for further miniaturization of circuit components. The thickness of SiO_2 layer has reached its limiting values beyond which the leakage current does not allow reliable device operation. HfO_2 is a candidate material for possible replacement of SiO_2 due to its achievable lower equivalent oxide thickness (EOT) which is the layer thickness corresponding to the same capacitance value with a thinner SiO_2 dielectric layer thickness. With a high-k dielectric constant, HfO_2 can be growth thicker to obtain capacitance values equivalent to those obtained with low dielectric materials such as SiO_2. This results in less leakage current and degradation effects in devices like flash memory cells. Thanks to the Fowler-Nordheim tunneling, HfO_2 also provides larger current for charging operation in these devices. Thus, HfO_2 is foreseen as a candidate dielectric material to improve the device performance in memory applications [1–3]. In addition, polysilicon floating gates are traditionally used in today's memory elements. Instead of continuous poly gate, the use of Si nanocrystals as the storage medium has recently been investigated intensively. In these applications, Si can also be replaced with Ge because of its superior band offset values with longer retention time.

The interface structure of poly/nanocrystal layer with underlying tunnel oxide and with the top lying control oxide plays very important role in the device operation. Many research groups have studied interfacial layer formations in Si/HfO_2 structure during both fabrication and annealing. Thermodynamically driven SiO_2/Si formation at Si/HfO_2 interface is usually observed on the substrate side of HfO_2 [4]. This may degrade the performance of device. Some methods such use of Hf buffer layer or nitridation to retard chemical reaction have already been developed to eliminate this kind of formations at the interface [5–7].

As in the case of Si/HfO_2 system, the chemical and structural properties of SiO_2/Ge/HfO_2 interfaces needs to be understood if this structure is to be used in memory applications. Some studies focusing on certain aspects of Ge/HfO_2 interface have already been reported [8,9]. Like in Si/HfO_2 case, surface nitridation was also studied to suppress any oxide formation at the interface of Ge/HfO_2. None of these research groups reported any structural/chemical details of the untreated interfaces of the entire SiO_2/Ge/HfO_2 multilayer structure.

In this study, we report XPS depth profiling of the interfaces in the SiO_2/Ge/HfO_2/Si multilayer structure. HfO_2 was chosen to be 10 nm which is thick enough to eliminate the Ge penetration on to the substrate. We particularly focused on the behavior of Ge layer during the fabrication and annealing processes. Oxidation and segregation of Ge atoms are typically observed at the Ge/HfO_2 interface after the annealing process at 800 °C.

2. Experimental Procedure

SiO_2/Ge/HfO_2 structures with 10 nm HfO_2 high-k dielectric was fabricated on p-type Si (100) substrate by sputtering technique. HfO_2 acts as the tunnel oxide of the memory cell composed of this

* Corresponding author. Department of Applied Physics, Eindhoven University of Technology, 5600 MB Eindhoven, The Netherlands.
E-mail address: sahin.dondu@gmail.com (D. Sahin).

0040-6090/$ – see front matter © 2009 Elsevier B.V. All rights reserved.
doi:10.1016/j.tsf.2009.09.156

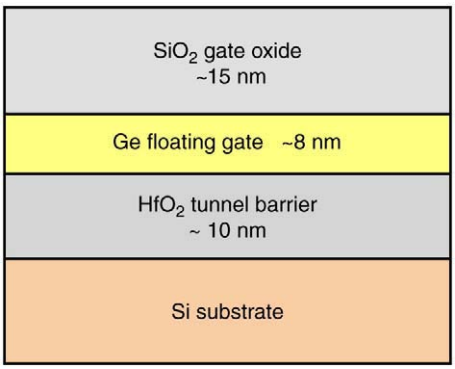

Fig. 1. Schematic representation illustrates the cross sectional view of cell.

multilayer. As the floating gate and control dielectric, Ge and SiO_2 layers were grown on HfO_2 films by sputtering at room temperature. The grown layer is shown in Fig. 1 schematically. The thicknesses of Ge and SiO_2 layers were measured to be ~8 nm and ~15 nm by thickness monitor of the deposition system, respectively. Growth process is conducted at room temperature.

Chemical structure and interfacial properties of grown structure were studied before and after the heat treatment. Annealing was performed at 800 °C in N_2 ambient for 30 min in cleanroom conditions. *Ex-situ* X-ray Photoelectron Spectroscopy (XPS) is used to analyze trilayer stack structure. XPS measurements were done with SPECS EA-200 system, using an Al Kα X-ray source ($h\gamma = 1486.6$ eV). About 60 layers were sputtered with Ar ion gun operating at 2500 eV to analyze all stacks for both as-sputtered and annealed samples. There was no observable carbon contamination in the films after removal of the first layer for 2 min Ar sputtering. Depth profiling was started after the removal of this top layer. The XPS data were processed after Shirley background substraction by using both PeakFit™ and XPSPEAK programs.

Raman spectroscopy measurements were conducted for samples to understand the crystallinity of the Ge layer. Measurements were employed in backscattering geometry using 632.8 nm light source of a conformal micro-Raman (HR800, Jobin Yvon) system, attached with Olympus microanalysis unit and a liquid-nitrogen-cooled CCD camera providing a resolution of ~1 cm^{-1}. Measurements were conducted at room temperature.

3. Results

SiO_2/Ge/HfO_2/Si multilayer structure was analyzed using XPS depth profiling technique with 60 sputtering steps. Each sputtering step corresponds approximately to the removal of ~3–4 nm layers. The actual values vary for different materials and their micro structure. Fig. 2 shows representative XPS spectra and deconvoluted peaks of Si, Ge and Hf and their chemical states at two different locations for the sample annealed at 800 °C in nitrogen ambient. Deconvolution process was performed using Shirley background subtraction method which is generally accepted to be the best technique for this process. In Fig. 2 (a), the upper curve belongs to the Si 2p signal that is obtained from the Si substrate reached after 50 sputtering cycles, whereas the lower curve is from the top SiO_2 layer. These two signals measured at 99.2 eV and 103.7 eV corresponds to the typical Si and SiO_2 peak positions, respectively. There are no significant shifts observed at peak positions of Si and SiO_2. The small peak seen at around 94 eV is the satellite peak of Si originated from ionization of X-ray photons with slightly higher energies.

Ge 3d signal displayed in Fig. 2 (b), exhibiting double peak features, results from the pure Ge and the GeO_x state. After 20 sputtering cycles, Ge 3d peak is dominated by the pure Ge signal located at 29.3 eV. GeO_x signal (at 32.3 eV) is detectable as approached to Ge/HfO_2 interface and when we approach further towards the Ge/HfO_2 interface, the binding energy peak corresponding to GeO_x signal dominates over the pure Ge signal.

Hf 4f peaks are shown in Fig. 2 (c) in a similar way for two different layers with different chemical form of Hf molecule. Lower curve in this figure shows Hf signal obtained from cycle 33 as a representative example. After 26th sputtering cycle, Hf peaks corresponding to these spin states were measured with binding energy of 17.6 eV and 19.3 eV that can be assigned to the peak position of HfO_2 [8]. Hf 4f signal is typically composed of two main peaks, ($4f_{5/2}$ and $4f_{7/2}$) split due to

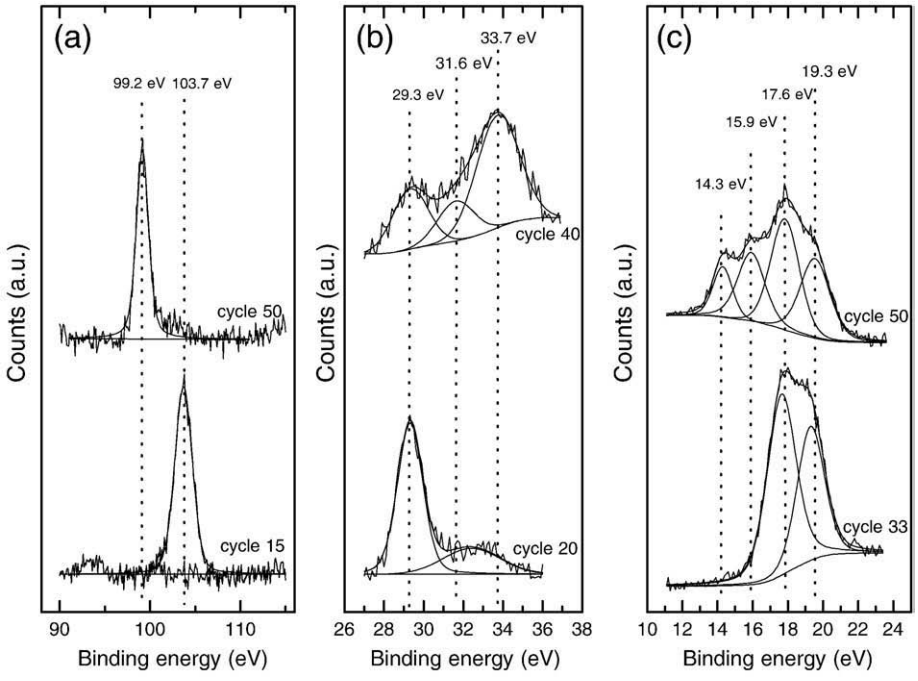

Fig. 2. XPS spectra of Si (a), Ge (b) and Hf (c) after annealing at 800 °C in N_2 ambient for 0.5 h.

spin orbit interaction. When we approach to the interface with the Si substrate, two additional peaks emerge at 15.9 eV and 14.3 eV (upper curve of Fig. 2 (c)). These two peaks appearing at the HfO_2/Si interface are resulted from HfSi/$HfSiO_x$ and Hf with low oxygen content. It should be mentioned that the presence of pure Hf metal, which might be in the form of local nanocluster, or HfSi regions without any oxygen content since this cannot be excluded from the XPS signal alone as the peak position of these formation is hardly distinguishable [6,8–11].

Behavior of Ge at the interface of SiO_2/Ge and Ge/HfO_2 is of great interest because the electronic properties of these interface states, which play crucial role in the device operation, are mainly determined by the chemical formations there. A complete evolution of Ge 3d peak across the multilayer structure is displayed as three dimensional graphs in Figs. 3 and 4, before and after the annealing processes, respectively. Presence of pure and oxidized Ge is clearly distinguishable in both figures. While GeO_x is observed only at the HfO_2/Ge interface of as fabricated sample, it is also seen at Ge/SiO_2 interface after annealing at 800 °C in nitrogen ambient. It appears that Ge atoms close to the Hf interface are oxidized during the deposition. It is likely that Ge atoms extract O atoms from the underlying HfO_2 film. The charge carrier should tunnel through the Ge/HfO_2 interface during the write/erase operation in a flash memory element and the presence of GeO_x influences the electronic barrier determining the tunneling process at the interface. Thus, formation of Ge oxide at the HfO_2/Ge interface should be taken into account during the device design and analysis.

Depth profiling of all elements across the stacked multilayer structure before and after annealing is shown in Fig. 5. Interfaces separated into four fundamental regions that are as indicated in the figure. We see that the top SiO_2 layer formed by magnetron sputtering is almost stoichiometric and pure. Carbon contamination is observed only at the very beginning surface layers. It was detected that HfO_2 film layer was containing a large amount of Ge before annealing. It seems that while Ge atoms penetrate into the underlying HfO_2 layer during the sputtering process, the annealing process greatly reduces the Ge amount in the HfO_2 film. The stoichiometry of the HfO_2 film is then healed by out diffusion of Ge atoms. The segregation of Ge from SiO_2 is a commonly observed phenomenon [12,13]. Similar behavior was also reported for Ge in the Al_2O_3 matrix [14]. We observed that Ge atoms behave in a similar way in HfO_2. This effect is apparently related to the low solubility of Ge in the oxide materials.

In order to analyze the chemical state of constituting elements across the SiO_2/Ge/HfO_2/Si stacked structure, binding energy values of Ge 3d and Hf 4f were extracted by a careful deconvolution process such as plotted in Fig. 6. It was also shown in this figure how these chemical states changed during the annealing. In Fig. 6 (a) and (b),

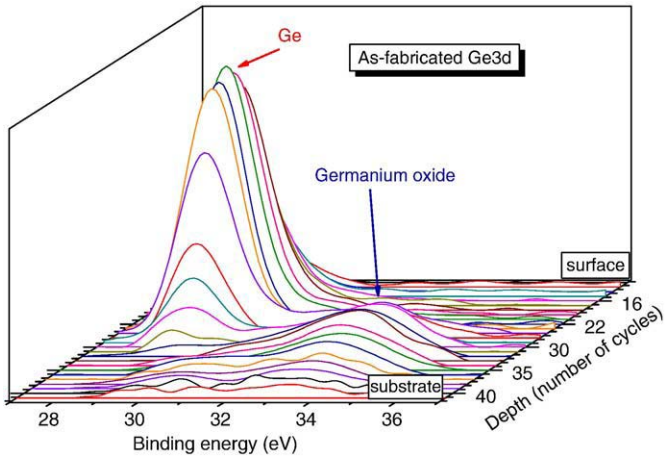

Fig. 3. Smoothed data obtained from as-fabricated-Ge 3d peak position beginning from cycle 12 to 51. Ge signal started to be collected after cycle 12 to 40.

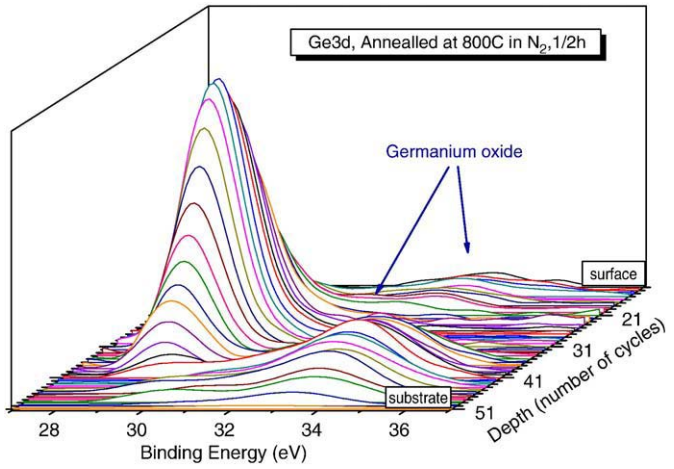

Fig. 4. Smoothed data showing the peak positions of Ge 3d for annealing at 800 °C.

peak positions of Ge 3d and Hf 4f are shown, respectively. Binding energy values of Ge 3d peak positions were 29.3, 31.2 and 33.6 eV corresponding to Ge^0, GeO_x and GeO_2.The peak assigned to GeO_x could not be resolved any further due to the weak signal intensity. We see from Fig. 6 (a) that Ge was oxidized at the interface of HfO_2 even before the annealing process. It seems that Ge atoms were oxidized by the oxygen atoms provided by the underlying HfO_2 layer during the sputtering. Upon annealing at 800 °C, the other edge of the Ge film on SiO_2 interface got oxidized, too. This oxidation took place with the oxygen atoms available in trace amounts in the annealing ambient even though the annealing was carried out in high purity nitrogen gas ambient under clean room conditions. We see however from Figs. 3, 4 and 6a, a significant amount of pure Ge remained intact even after the annealing process at 800 °C.

The situation is more complicated for Hf, due to the presence of different phases and to spin-orbit splitting of the peaks. By using the deconvolution process described above, we were able to determine the chemical states shown in Fig. 6 (b) with some uncertainty. Fig. 6 (b) suggests that even HfO_2 layer is mostly in the oxide form before annealing, some unoxidized Hf atoms are detectable at HfO_2/Si interface. The peak measured at 17.6 eV corresponds to the fully stoichiometric HfO_2 $4f_{7/2}$ signal ($4f_{5/2}$ is 1.6 eV larger than this value) while the slightly shifted peak at 16 eV can be attributed to either HfSi or $HfSiO_x$. Previous publications on HfO_2/Si systems suggest the presence of both phases [15,16]. As we measure a strong oxygen signal from the same region (not shown here), it is more likely that this part of the structure is composed of $HfSiO_x$ rather than HfSi. The relative intensities of HfO_2, Hf, and HfSi/$HfSiO_x$ obtained after peak fit show that this region is highly dominated by HfO_2 although other chemical formations are present.

As complementary technique, we performed Raman spectroscopy measurements to identify the presence of Ge–Ge bonds and their evolution with respect to annealing. Fig. 7 shows the Raman spectra for as grown and annealed samples. In addition, we have included data from samples annealed at other temperatures. As expected Ge–Ge peak located at 299.6 cm^{-1} emerged in the spectra after annealing at 700 °C and 800 °C. We show that the peak intensity is maximum for the samples annealed at 700 °C, and decreases with increasing temperature. This is clearly a result of the increase in Ge oxidation with the temperature. This result agrees very well with the XPS results (Figs. 3 and 4) for the 800 °C annealed samples where partial oxidation of Ge atoms is observed. In addition, it should be also mentioned that precipitation of Ge on the Si substrate might have reduced the Raman intensity with temperature. Although not documented in this study, this effect is well known for Ge/SiO_2 systems and possibly observable for the Ge/HfO_2 structures.

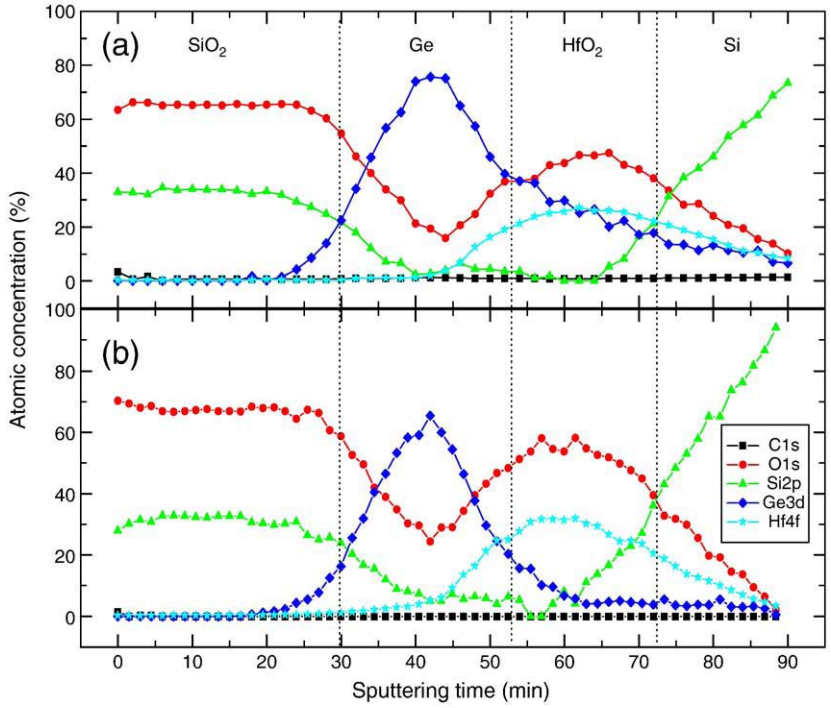

Fig. 5. Depth profiling spectra of SiO_2/Ge/HfO_2/Si specimen for (a) as growth and (b) annealed at 800 °C in highly pure nitrogen ambient.

One further feature observed in the Raman spectra is the shoulder appearing in the lower wave number side of the main peak of the sample annealed at 700 °C. A shift in the Raman peak towards the lower wave numbers has been attributed to quantum size effect. A presence of such a shoulder is then an indication of nano-sized structure. In our earlier publication, we showed that the size of Ge nanocrystals can be estimated from the asymmetric Ge peak [17]. The annealing temperature of 700 °C is lower end of the temperature range in which Ge crystallization occurs. We would then expect some regions of the film has been partially crystallized and have nanocrystals rather than a continuous film. Consistently, we detect that the shoulder disappears when the sample is annealed at higher temperatures.

4. Conclusions

In summary, we demonstrated the chemical structure and interfacial properties of SiO_2/Ge/HfO_2/Si multi-stack structure. *Ex-situ* XPS depth profiling and Raman analysis were employed for interface characterization and Ge crystalline structure determination, respectively. It is observed by XPS that after annealing at 800 °C in

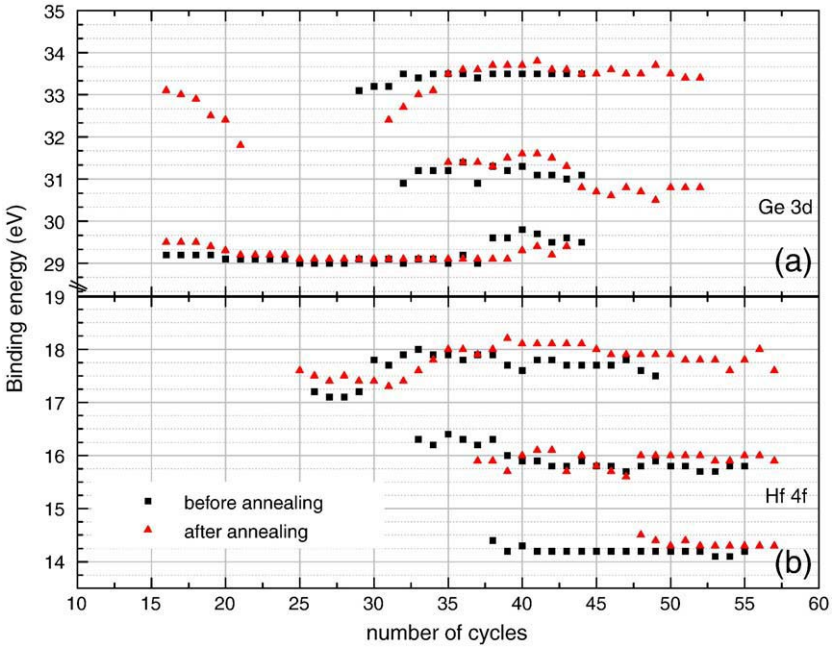

Fig. 6. Peak positions of Ge (a) and Hf (b) before and after annealing processes.

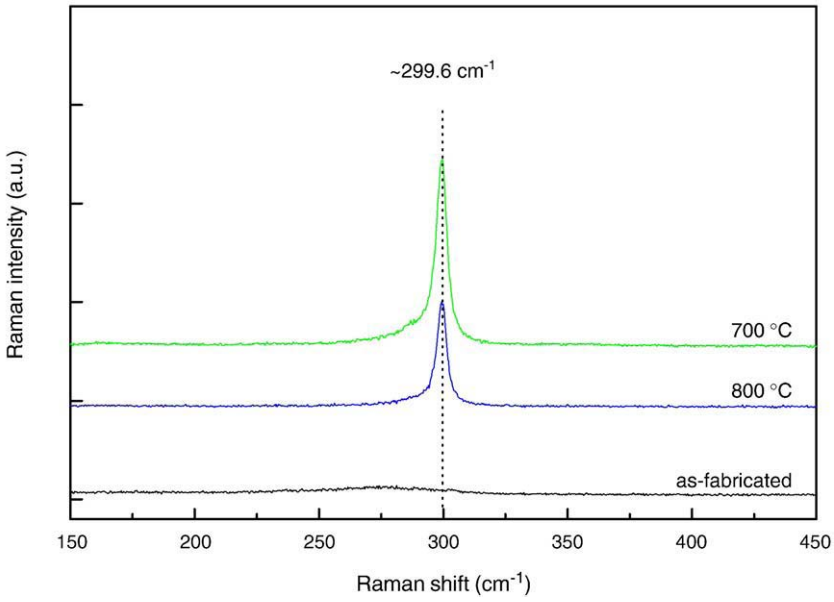

Fig. 7. Raman spectra of as growth and annealed samples in nitrogen ambient at various temperatures.

nitrogen ambient for half an hour, Ge is segregated out from HfO_2 and oxidized at SiO_2 interface. In addition, Hf metal and $HfSi/HfSiO_x$ formations are observed at HfO_2/Si interface.

Acknowledgements

The authors would like to thank the Department of Microtechnology and Nanoscience (MC2), Chalmers University of Technology for providing support for the preparation of HfO_2 layers at MC2 as a part of EU Research Infrastructure (RI) project. This work was partially supported by Turkish Research Council (TUBITAK).

References

[1] S.J. Lee, H.F. Luan, C.H. Lee, T.S. Jeon, Y. Senzaki, D. Roberts, D.L. Kwong, IEDM Tech. Dig. (2000) 31.
[2] T.H. Ng, W.K. Chim, W.K. Choi, V. Ho, L.W. Teo, A.Y. Du, C.H. Tung, J. Appl. Phys. Lett. 84 (2004) 4385.
[3] S. Wang, W. Liu, Appl. Phys. Lett. 86 (2005) 113105.
[4] G. Aygun, I. Yildiz, J. Appl. Phys. 106 (2009) 014312.
[5] S.K. Stanley, S.V. Joshi, S.K. Banerjee, J.G. Ekerdt, J. Vac. Sci. Technol. A. 24 (2006) 78.
[6] R. Tan, Y. Azuma, I. Kojima, Surf. Interface Anal. 38 (2006) 784.
[7] J.H. Lee, K. Koh, N.I. Lee, M.H. Cho, Y.K. Kim, J.S. Jeon, K.H. Cho, H.S. Shin, M.H. Kim, K. Fujihara, H.K. Kang, J.T. Moon, IEEE Int. Electron Devices Meet. Tech. Dig. (2000) 645.
[8] S. Toyada, J. Okabayashi, H. Kumigashira, M. Oshima, K. Omo, M. Niwa, K. Usuda, G.L. Liu, Appl. Phys. Lett. 84 (2004) 2328.
[9] M. Gutowski, J.E. Jaffle, C-L Liu, M. Stoker, Appl. Phys. Lett. 80 (2002) 1897.
[10] A. Zenkevich, Y. Lebedinskii, G. Scarel, M. Fanciulli, A. Baturin, N. Lubovin, Microelectron. Reliab. 47 (2007) 657.
[11] S. Toyoda, J. Okabayashi, H. Kumigashira, M. Oshima, A. Ono, M. Niwa, K. Usuda, G.L. Liu, Symp. VLSI Tech. Dig. (2006) 14.
[12] R. Turan, T.G. Finstad, Semicond. Sci. Technol. 7 (1992) 75.
[13] E.S. Marstein, A.E. Gunnæs, A. Olsen, T.G. Finstad, R. Turan, U. Serincan, J. Appl. Phys. 96 (2004) 4308.
[14] S. Yerci, M. Kulakci, U. Serincan, R. Turan, M. Shandalov, Y. Golan, J. Nanosci. Nanotechnol. 8 (2008) 759.
[15] R. Tan, Y. Azuma, I. Kojima, Surf. Interface Anal. 38 (2006) 784.
[16] T.P. Smirnova, V.V. Kaichev, L.V. Yakovkina, V.I. Kosyakov, S.A. Beloshapkin, F.A. Kuznetsov, M.S. Lebedev, V.A. Gritsenko, Inorg. Mater. 44 (2008) 965.
[17] U. Serincan, G. Kartopu, A.E. Gunnæs, T.G. Finstad, R. Turan, Y. Ekinci, S.C. Bayliss, Semicond. Sci. Technol. 19 (2004) 247.